JOURNAL OF AIRCRAFT
Vol. 34, No. 4, July–August 1997

Lateral Escape Guidance Strategies for Microburst Windshear Encounters

H. G. Visser*
Delft University of Technology, Delft 2600 GB, The Netherlands

This paper presents the outcome of a preliminary research effort involving the development of a near-optimal lateral escape guidance technique for aircraft encountering a microburst on final approach. The proposed guidance technique relies either on in situ or on relatively short-range forward-look windshear detection. Simulated guidance solutions are evaluated in terms of recovery-altitude performance and robustness to uncertainty in microburst size and strength. Based on a comparison with exact open-loop optimal solutions, the employed technique of directing the aircraft toward a target recovery altitude constitutes itself as a very promising longitudinal guidance strategy. The lateral escape strategy, though very simple, also proved to be very effective, reconfirming the overall benefits of lateral escape vis-á-vis nonturning escape. Before a practical implementation of the guidance strategies can take place, several issues still need be addressed. This paper briefly outlines the missing elements to provide a framework for future research and development.

I. Introduction

LOW-LEVEL windshear phenomena, particularly microbursts, have long been recognized as potential hazards to aircraft, especially during takeoff or approach-to-landing. Upon encountering a microburst in a glide-slope approach, a pilot has essentially two options: to abort the landing or to proceed. If the altitude at which the windshear warning is received is sufficiently high, aborting the approach is the safer procedure. Since we seek to avert an impending crash, a natural choice for the objective in such an aborted approach-to-landing is the maximization of the terrain clearance, or in other words, the maximization of the minimum altitude at any point along the escape trajectory. An equivalent specification of this performance measure is to minimize the peak value of altitude drop, i.e., the difference between a constant reference altitude h_{ref} and the instantaneous altitude (Fig. 1).

In earlier work involving open-loop trajectory optimization,[1,2] this so-called minimax (or Chebyshev) performance index was approximated by a Bolza integral performance index. However, in more recent work,[3] exact Chebyshev solutions could be established by transforming the minimax problem into an equivalent optimal control problem with state variable inequality constraints. It was shown that, effectively, the transformation technique amounts to enforcing a minimum altitude constraint $h \geq h_{\min}$, while maximizing the minimum altitude limit $h_{\min}$.

A comparison of solutions based on the Bolza performance index approximation (Bolza solutions) with the solutions to the original minimax problem (Chebyshev solutions), revealed not only a marked improvement in reducing the peak value of altitude drop, but perhaps even more significant is that the overall longitudinal behavior is radically different. On the other hand, the difference in lateral behavior between Chebyshev and Bolza solutions is modest. Generally speaking, it can be observed that in the final stage of a lateral escape maneuver (i.e., in the after-shear region), an aircraft ends up flying along a horizontal wind radial. Based on this behavior, a lateral escape strategy in combination with a simple constant-pitch technique was proposed in Ref. 4. The behavior of the simulated guidance solutions in Ref. 4 showed a remarkable degree of agreement with the Bolza solutions. However, in view of the observation made earlier, this in turn implies that the performance and longitudinal behavior of the simulated guidance solutions do not closely approximate that of the Chebyshev solutions established in Ref. 3. The main purpose of the present preliminary study is to explore alternative guidance laws that offer improved performance. In particular, we seek to replace the constant-pitch guidance technique by an alternative longitudinal guidance law.

Open-loop optimal solutions are based on global information of the wind flowfield. Indeed, in an open-loop Chebyshev solution, the actual achieved recovery altitude during a microburst encounter is such that the angle of attack just reaches its limit as the high-shear region is exited. In a real-world situation, however, a fair degree of uncertainty with respect to the intensity and extent of the windshear is inevitable, even if advanced forward-sensing technology is deployed. Consequently, when a microburst is encountered, a pilot is generally unsure where and when the high-shear region will end. To make an aircraft less vulnerable to uncertainties in microburst size and strength, a pilot may attempt to limit the energy drain caused by windshear, such as trying to reduce the risk of premature angle-of-attack saturation. Unfortunately, any attempt to increase specific energy at the termination of the encounter typically comes at the expense of a lower recovery altitude and, therefore, a compromise between the two conflicting requirements must be made. To permit a tradeoff between recovery altitude and energy management, a composite performance measure was introduced in Ref. 3, consisting of a weighted combination of the minimax criterion and the maximum final energy criterion. The open-loop optimal control results established in Ref. 3, based on the composite criterion, serve here as ideal standards, against which simulated closed-loop guidance solutions can be compared.

II. Microburst Encounter Modeling

To formulate the equations of motion, we make use of a moving, but nonrotating reference frame, translating with the local air mass (relative wind-axes reference-frame). With the usual premises,[3] the equations of motion describing

Received Oct. 9, 1996; presented as Paper 97-0535 at the AIAA 35th Aerospace Sciences Meeting, Reno, NV, Jan. 6–9, 1997; revision received April 14, 1997; accepted for publication April 15, 1997.

*Lecturer, Faculty of Aerospace Engineering. Senior Member AIAA.

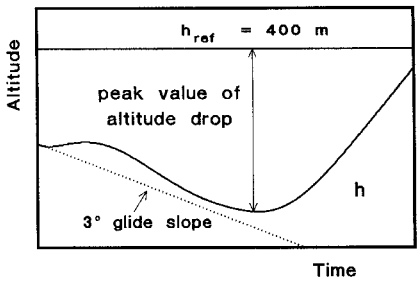

Fig. 1 Illustration of minimax performance index.

the dynamics of a point-mass-modeled vehicle, moving in three-dimensional space, can be written as follows:

$$\dot{x} = V\cos\gamma\cos\psi + W_x \tag{1}$$

$$\dot{y} = V\cos\gamma\sin\psi + W_y \tag{2}$$

$$\dot{h} = V\sin\gamma + W_h \tag{3}$$

$$\dot{E} = \frac{(\beta T_{\max}\cos\delta - D)V}{W} + \dot{W}_h - \frac{V}{g}(\dot{W}_x\cos\gamma\cos\psi + \dot{W}_y\cos\gamma\sin\psi + \dot{W}_h\sin\gamma) \tag{4}$$

$$\dot{\gamma} = \frac{g}{V}\left(\frac{L + \beta T_{\max}\sin\delta}{W}\cos\mu - \cos\gamma\right) + \frac{1}{V} \times (\dot{W}_x\sin\gamma\cos\psi + \dot{W}_y\sin\gamma\sin\psi - \dot{W}_h\cos\gamma) \tag{5}$$

$$\dot{\psi} = \frac{g}{V\cos\gamma}\frac{L + \beta T_{\max}\sin\delta}{W}\sin\mu + \frac{1}{V\cos\gamma}(\dot{W}_x\sin\psi - \dot{W}_y\cos\psi) \tag{6}$$

$$\dot{\beta} = \frac{1}{\tau}(\beta_t - \beta) \tag{7}$$

where x, y, and h are the position coordinates, E is the specific pseudoenergy, γ is the flight path angle, ψ is the heading angle, and β is the throttle response. The wind velocity vector has components, W_x, W_y, and W_h. The thrust is assumed to have a fixed inclination δ relative to the zero-lift axis. The throttle response is modeled as a first-order lag with a time constant τ.

Note that specific pseudoenergy E is formally defined as[5]

$$E \triangleq h + (V^2/2g) \tag{8}$$

In this definition, potential energy (i.e., altitude h) is an inertial quantity; whereas kinetic energy (i.e., $V^2/2g$) is referenced relative to the moving air mass. This is the reason why E is actually called pseudoenergy. Although it is certainly possible to define kinetic energy in terms of inertial speed, it is the energy relative to the air mass that is really the key quantity in an aborted approach-to-landing. Indeed, airspeed is the all-important state in a microburst encounter when it comes to avoiding stall. For reasons of simplicity, E is called (specific) energy rather than pseudoenergy throughout this paper.

The three control variables in the system model are all subject to inequalities:

$$0 \le \beta_t \le 1 \tag{9}$$

$$|\mu| \le \mu_{\max} \tag{10}$$

$$0 \le \alpha \le \alpha_{\max} \tag{11}$$

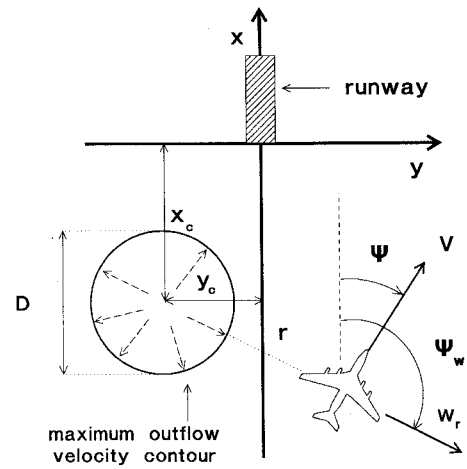

Fig. 2 Geometry of microburst encounter.

where β_t is the throttle setting, μ is the bank angle, and α is the angle of attack.

The aerodynamic forces (lift L and drag D) are modeled in the usual fashion:

$$L = C_L(\alpha)\tfrac{1}{2}\rho V^2 S, \qquad D = C_D(\alpha)\tfrac{1}{2}\rho V^2 S \tag{12}$$

The maximum available thrust force $T_{\max}$ is assumed to be a function of airspeed only. The aircraft type used in the investigation is a Boeing 727. Details of the aerodynamic and thrust data for this particular aircraft type (in landing configuration) can be found in Ref. 3. In this study, we also employ the microburst model described in Ref. 3.

In view of the axisymmetric character of the employed microburst model, polar coordinates have been used to describe the wind flowfield in a horizontal plane (Fig. 2). The use of polar coordinates allows the horizontal wind components W_x and W_y to be readily evaluated in terms of the radial wind velocity W_r and the direction of the radial wind velocity vector $\boldsymbol{\psi}_w$:

$$W_x = \cos\boldsymbol{\psi}_w W_r(r), \quad W_y = \sin\boldsymbol{\psi}_w W_r(r) \tag{13}$$

An important metric used in the evaluation of windshear performance is the F-factor. The F-factor represents a direct measure of the degradation of an aircraft's capability to gain energy because of the windshear. Similar to Ref. 3, the F-factor is defined here as

$$F \triangleq [(T - D)/W] - (\dot{E}/V) \tag{14}$$

III. Exact Open-loop Optimal Solutions

In this section, some of the major findings established in Ref. 3 are reiterated, primarily for the purpose of extracting the essential features of open-loop optimal trajectories. First, we formally restate the performance index that we seek to optimize. As already pointed out in the Introduction, the primary objective in this study is to minimize the peak value of the altitude drop. This Chebyshev minimax performance index will be denoted here as J_2:

$$J_2 = \{\max_t [h_{\text{ref}} - h(t)]\}, \qquad 0 \le t \le t_f \tag{15}$$

where t_f is the (fixed) flight time. The other major criterion considered in Ref. 3 concerns the maximization of specific energy at termination:

$$J_3 = -E(t_f) \tag{16}$$

The minus sign in Eq. (16) stems from the fact that we seek

to minimize the performance index J_3. To permit a tradeoff between the various performance criteria, the following composite index is considered:

$$\bar{J} = \int_0^{t_f} \left(1 - \frac{h}{h_{\text{ref}}}\right)^6 \mathrm{d}t + K_1\{\max_t[h_{\text{ref}} - h(t)]\} - K_2E(t_f)$$
$$= J_1 + K_1J_2 + K_2J_3 \tag{17}$$

where K_1 and K_2 are (positive) weight factors. Note that J_1 represents the Bolza functional that approximates the Chebyshev index (15), originally used in Refs. 1 and 2.

With the parameter K_2 set equal to zero in the performance index, the optimization of recovery altitude is addressed. The weight factor K_1 then more or less serves as an interpolation parameter between the Bolza solution ($K_1 = 0$) and the Chebyshev solution ($K_1 \to \infty$). The following numerical example, which is taken from Ref. 3, serves to illustrate the influence of the weight factor K_1 on the solution behavior of lateral escape trajectories. In the considered scenario, the center of the microburst is located on the runway centerline extension, 1.5 km from the runway threshold. The aircraft initial state corresponds to a situation in which an aircraft would fly during a stabilized approach along the glide slope at 2.5 km from the runway threshold. It is noted that for the considered microburst size and location, the aircraft position at which the escape is commenced is on the maximum radial outflow velocity contour. From an operational perspective, the assumed scenario is therefore representative of an encounter featuring in situ windshear detection. The bank angle limit has been set at 10 deg in this particular example. Obviously, full throttle is applied during an escape maneuver, such as to maximize the specific energy rate.

Figure 3 presents results pertaining to three different values of K_1, viz., $K_1 = 0$, 0.025, and 25. The case $K_1 = 0$ represents the original Bolza problem; whereas for $K_1 = 25$, a virtually pure Chebyshev problem is obtained. Figure 3a shows the ground tracks of the resulting optimal escape trajectories. Inspection of Fig. 3b shows that the overall angle-of-attack behavior for $K_1 = 0$ and $K_1 = 0.025$ is very similar. Nevertheless, the resulting altitude profiles are quite different (Fig. 3c). In particular, the achieved recovery altitude is significantly higher for the trajectory computed with $K_1 = 0.025$. Furthermore, it is noted that a further massive increase in the parameter K_1 (from $K_1 = 0.025$ to $K_1 = 25$) leads to only a modest additional improvement in minimum altitude. However, the angle-of-attack behavior is markedly different for the latter case, especially in the initial phase of the encounter. As a result, altitude is rapidly traded for speed in the Chebyshev solution.

In the second example, which is based on the same scenario as the first example, the energy end-cost function is assessed. Now a fixed value for K_1 is adopted, while the factor K_2 is parametrically varied. If the factor K_2 is only slightly increased from zero, the impact on the solution will only become notable in the final seconds of the flight, well outside the high-shear region (Fig. 4). However, as the weighting of the final specific energy term in the composite performance index is increased, the overall trajectory behavior is influenced in the sense that altitude performance is sacrificed for the sake of gaining specific energy. Indeed, by descending to a low level the aircraft is placed in a region of relatively low downdraft.[6]

If an aircraft descends below the best recovery altitude that is theoretically achievable in a Chebyshev solution, an additional survival capability can be obtained in the form of an airspeed (kinetic energy) reserve. The largest airspeed reserve

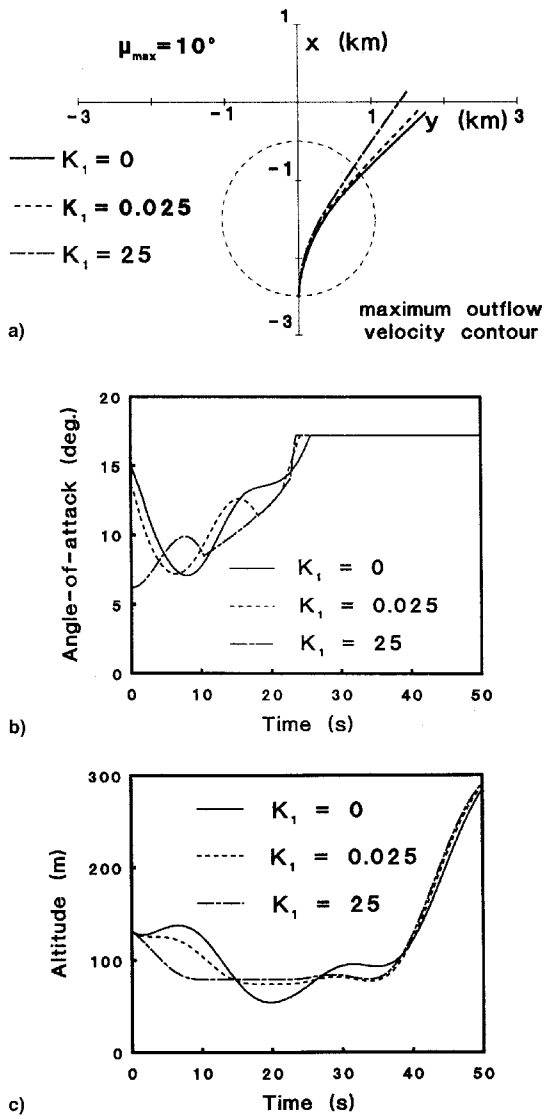

Fig. 3 Comparison of extremal solutions for various values of K_1. $K_2 = 0$; lateral maneuvering ($\mu_{\max} = 10$ deg).

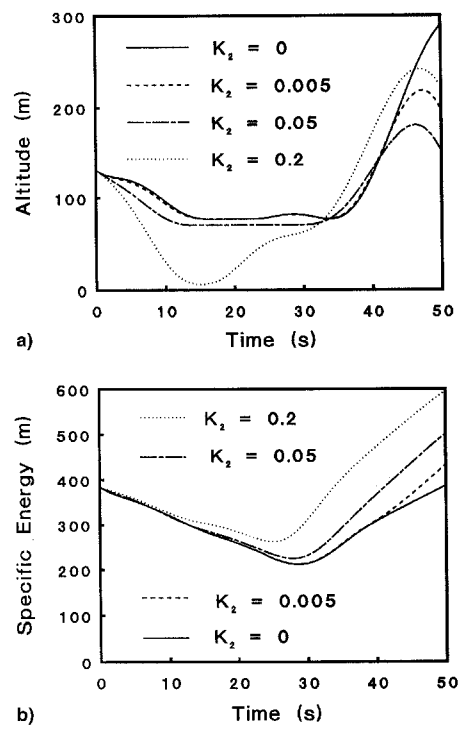

Fig. 4 Comparison of extremal solutions for various values of K_2. $K_1 = 0.05$; lateral maneuvering ($\mu_{\max} = 10$ deg).

is obtained by descending to the lowest allowable altitude in terms of obstacle clearance. The question is whether it is really wise to always descend to this minimum safe altitude. If this procedure is executed in moderate windshear, an aircraft may end up flying at high speed, close to the deck. Descending to an altitude level above the minimum safe altitude is then probably a safer procedure. In turn, opting for the latter technique results in the question of how to select an appropriate target altitude. If the target altitude is selected too high, the stick shaker may activate well before the shear region is exited, an event generally resulting in dramatic altitude loss. Only if the intensity and extent of the microburst can be properly estimated onboard (forward-look sensing), does there appear to be some hope for devising appropriate (preferably adaptive) logic for the selection of the target altitude.

IV. Closed-Loop Guidance Approximations

A new longitudinal guidance law has been derived as an alternative for the constant-pitch technique, employed in earlier work.[4] The derivation of the guidance law closely follows the lines of Ref. 7, as far as the outer control loop is concerned. The technique described in Ref. 7 for synthesizing the inner control loop (for the fast rotational dynamics) is also very interesting, and is a topic currently being pursued.

The employed closed-loop guidance synthesis is based on the technique of dynamic inversion.[8] The essence of dynamic inversion is to find a nonlinear transformation of variables (via the introduction of so-called pseudocontrols), through which a nonlinear system can be transformed into a linear system. Subsequently, a relatively simple control law can be developed that gives the linear system the desired characteristics, after which an inverse transformation takes place to the original variables. The method is particularly useful for determining the control input histories (feedforward control) to obtain desired outputs. This is only part of the control design, since feedback control is almost always necessary for a satisfactory implementation. However, feedback is mainly used to provide or augment stability, and to handle disturbances and model inaccuracies.

For lateral guidance, the simple law as presented in Ref. 4 has been retained here. From the behavior of the optimal trajectories, it was inferred in Ref. 4 that the guidance law for the commanded bank angle μ_c should take the following simple form:

$$\mu_c = K_\mu(\psi_w - \psi), \qquad |\mu_c| \le \mu_{\max} \tag{18}$$

with the gain coefficient K_μ selected as 0.25, and where it is understood that

$$-180 \le \psi_w \le 180 \text{ deg}, \qquad -180 \le \psi \le 180 \text{ deg} \tag{19}$$

The guidance law for the bank angle attempts to close the heading error, where heading error is defined as the relative (horizontal) wind direction. Note that in the headwind (entry) phase of the microburst encounter, the heading error is large so that maximum bank angle will be commanded. Only when the heading error has been closed sufficiently, i.e.,

$$|\psi_w - \psi| \le (\mu_{\max}/K_\mu) \tag{20}$$

will the bank angle start to decay exponentially. By rewriting Eq. (6) in terms of polar coordinates

$$\dot{\psi} = \frac{g}{V\cos\gamma}\frac{L + \beta T_{\max}\sin\delta}{W}\sin\mu + \left(\frac{\partial W_r}{\partial r} - \frac{W_r}{r}\right)\sin(\psi - \psi_w)\cos(\psi - \psi_w) + \frac{W_r}{V\cos\gamma}\frac{\partial W_r}{\partial r}\sin(\psi - \psi_w) \tag{21}$$

it becomes clear that in the terminal phase of the encounter, heading behavior can be approximately described by

$$\dot{\psi} = K_\psi(\psi_w - \psi) \tag{22}$$

To support the development of the new longitudinal guidance strategy, a small angle approximation has been introduced in the equations of motion for the thrust vector components along and perpendicular to the airspeed vector; i.e., $\cos(\alpha + \delta) \approx 1 - \frac{1}{2}(\alpha + \delta)^2$ and $\sin(\alpha + \delta) \approx (\alpha + \delta)$.

In view of the simplicity of the employed synthesis method for the longitudinal guidance strategy, its description will be kept brief here. A more detailed account of the longitudinal guidance strategy is given in Ref. 6. The objective is to control altitude by inverting the aircraft dynamics. Differentiation with respect to the time of Eq. (3) yields

$$u_c \triangleq \ddot{h}(t) = V\cos\gamma\dot{\gamma} + V\sin\gamma + \dot{W}_h = g\left\{\sin\gamma\frac{T[1 - \frac{1}{2}(\alpha + \delta)^2] - D}{W} + \cos\gamma\frac{L + T(\alpha + \delta)}{W}\cos\mu - 1\right\} \tag{23}$$

where u_c is an artificially introduced pseudocontrol. Equation (23) relates u_c to a quadratic polynomial in α, which is the original control variable. Next, the form of control must be specified to obtain the desired altitude dynamics. Unlike Ref. 7, where proportional integral derivative (PID) control is used, only proportional derivative (PD) control is used here (for the time being). The longitudinal guidance law that we propose will be referred to as altitude guidance:

$$\ddot{h}(t) = u_c = -[2\zeta\omega_0\dot{h} + \omega_0^2(h - h_c)] \tag{24}$$

where h_c is the commanded altitude. By judiciously choosing the feedback gains, the altitude response of the aircraft can be shaped as desired, as long as no control saturation occurs.

After the pseudocontrol u_c has been evaluated, using Eq. (24), the result can be substituted in Eq. (23). Assuming that the bank angle command has been evaluated using Eq. (18), Eq. (23) allows α to be solved in closed form in terms of the state variables. Obviously, the resulting angle-of-attack command needs to be subjected to the constraint specified in Eq. (11).

In addition to the previous altitude guidance scheme, a climb-rate guidance scheme has also been considered:

$$\ddot{h}(t) = u_c = -K_h(h - h_c) \tag{25}$$

where h_c is the commanded climb rate. Similar to Ref. 7, the commanded climb rate has been scheduled in terms of an aircraft's instantaneous available climb performance:

$$h_c = K_E E \tag{26}$$

It is clear that the gain factor K_E in Eq. (26) determines how specific energy is shared between kinetic and potential energy.

The potential advantage of the climb-rate control technique in comparison to the altitude guidance technique is that, in a certain sense, it is adaptive. The altitude guidance technique will always transfer the aircraft to the commanded altitude, regardless of the strength of the actually experienced windshear. So if, for example, a microburst turns out to be milder than originally anticipated, the resulting specific energy savings are invested in kinetic energy, rather than in potential energy. On the other hand, if climb rate is commanded in terms of an aircraft's instantaneous available climb performance, the rate of descent will be lower in moderate windshear than it is

in severe windshear. Consequently, the lower the strength of the microburst, the higher the recovery altitude. Unfortunately, it has proved to be rather difficult to actually realize these potential benefits in a practical implementation of climb-rate guidance. Without elaborate gain scheduling (K_E), climb-rate guidance is hardly useful. Extensive simulation experiments[6] have revealed that it is rather difficult to come up with a single gain scheduling scheme that produces near-optimal results in a variety of scenarios (including different microburst locations and intensities, forward-look detection range, lateral and non-turning escapes, etc.). In contrast, altitude guidance demonstrated a remarkable degree of robustness. For this reason, climb-rate guidance (with $K_E = 0.5$) is presently only used during the climb-out phase, once the high-shear region has been passed.

V. Simulated Guidance Solutions

A simulation program has been set up that is capable of simulating various guidance techniques. In situ and/or forward-look sensing of windshear is provided, although measurements are assumed to be perfect. Forward-look detection is simulated by computing the wind vector and its spatial gradients at a single point along the flight path vector, located at a range R_{look} ahead of the aircraft. The F-factor prediction is then based on this advance wind information, in combination with the momentary aircraft state. The simulated windshear detection system contains two (input) parameters only, viz., the detection range R_{look} and the F-factor detection threshold F_{thres}. An escape maneuver is initiated as soon as the measured F-value exceeds this specified threshold value. To simulate a reactive detection system, R_{look} is specified as zero (in future simulation trials, possibly even slightly negative, to simulate a turbulence filter delay).

The simulation program contains a simple guidance scheme for maintaining a stabilized localizer/glide-slope approach for the flight phase prior to the windshear alert. A switch to the escape logic is made as soon as the predicted (measured) F-factor exceeds F_{thres}. This escape logic involves the lateral guidance law [Eq. (18)] and the longitudinal guidance law [Eq. (24)]. Once the high-shear region has been exited, climb-rate scheduling is engaged to move the aircraft away from its recovery altitude. In the numerical examples that will be presented, the following selection has been made for the two coefficients in Eq. (24): $\omega_0 = 0.25$ rad/s and $\zeta = 0.8$.

For reference purposes, results involving the constant-pitch technique in conjunction with the lateral guidance law [Eq. (18)] will be presented. The constant-pitch guidance is based on a target pitch angle

$$\alpha_c = \theta_{\text{ref}} - \gamma, \qquad 0 \le \alpha_c \le \alpha_{\max} \tag{27}$$

with θ_{ref} selected as 15 deg, as specified in the Windshear Training Aid (WTA).[9] In the present simulation effort, pitch guidance has always been based on a 15-deg reference pitch angle throughout the escape flight. However, depending on the aircraft type, different values for θ_{ref} may be attempted for improved results in future research.[10]

To illustrate the proposed guidance concept, this section is concluded with some numerical examples. Both in situ ($R_{\text{look}} = 0$ m) and short-range forward-look ($R_{\text{look}} = 250$ m) detection are considered. The value F_{thres} is taken as 0.04 for both sensors. This threshold value is actually fairly low in comparison with current design values. However, it needs to be realized that in the present study, the F-factor measurements are not contaminated by high-frequency turbulence signals, and nuisance alerts are therefore of no concern. In all scenarios, the same initial condition is used, but the microburst location is 250 m displaced in longitudinal direction in the forward-look sensing scenarios. Effectively, the selected scenarios are such that there is no initial glide-slope approach phase, but an escape commences right at the initial condition. The only reason for such a setup of the scenarios is to obtain a fair basis of comparison with the exact (Chebyshev) solutions. Table 1 summarizes the recovery altitudes of exact Chebyshev solutions that have been used in a quantitative assessment of the altitude guidance concept.

The four open-loop Chebyshev solutions shown in Table 1 have been approximated by simulated closed-loop guidance solutions, using the two aforementioned guidance techniques. The initial aircraft state is the same in all encounters as that considered in Sec. III. The results are presented in Figs. 5–7.

Table 1 Optimal recovery altitudes $h_{\min}$ of exact Chebyshev solutions

$R_{\text{look}} = 0$ m		$R_{\text{look}} = 250$ m	
$\mu_{\max} = 0$ deg	$\mu_{\max} = 10$ deg	$\mu_{\max} = 0$ deg	$\mu_{\max} = 10$ deg
74.9 m	80.0 m	93.4 m	109.5 m

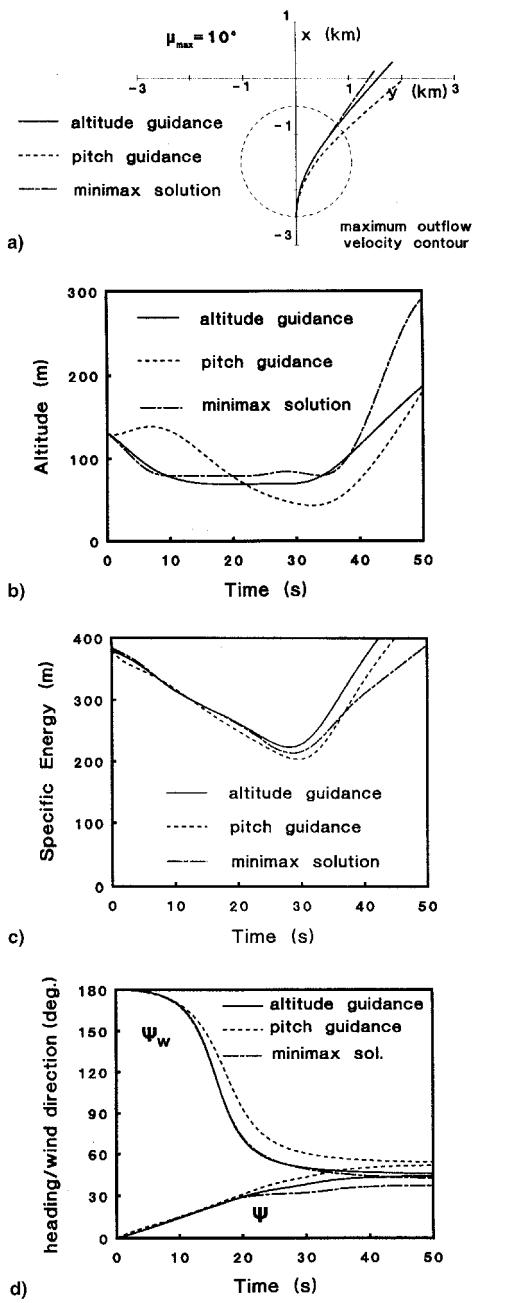

Fig. 5 Comparison of simulated guidance solutions with the extremal solution for a scenario involving in situ detection ($R_{\text{look}} = 0$ m). Lateral maneuvering ($\mu_{\max} = 10$ deg).

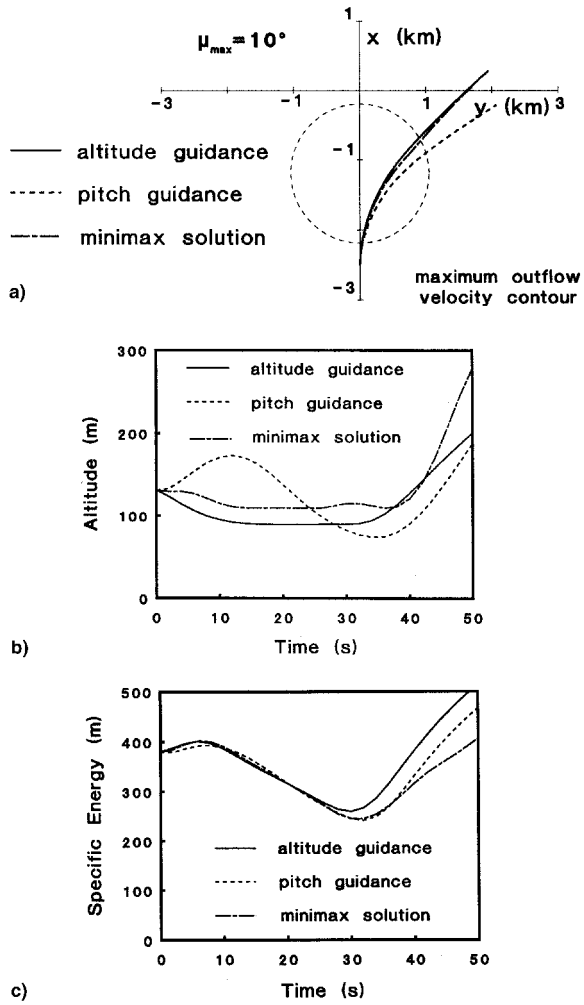

Fig. 6 Comparison of simulated guidance solutions with the extremal solution for a scenario involving forward-look detection (R_{look} = 250 m). Lateral maneuvering (μ_{max} = 10 deg).

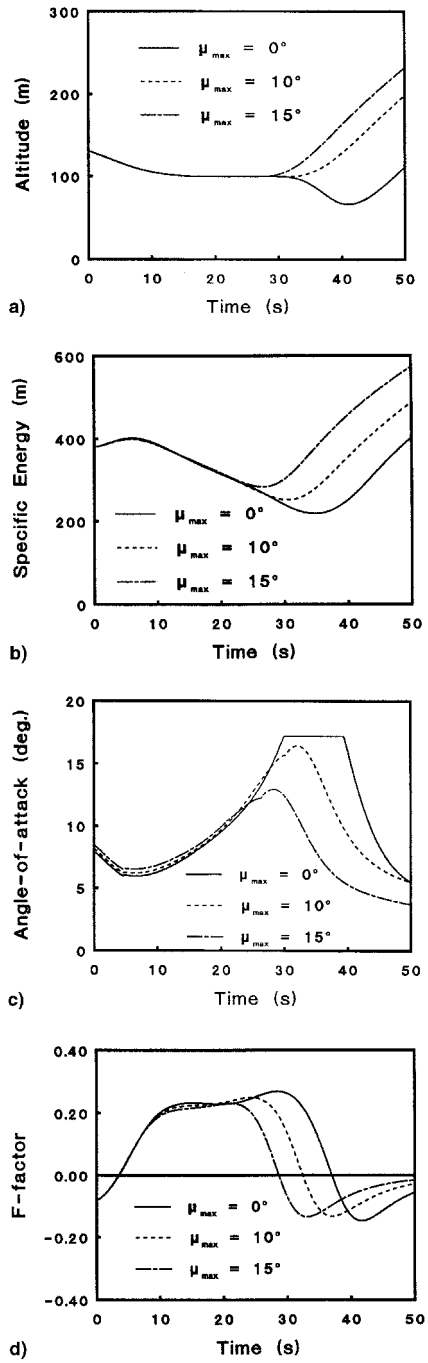

Fig. 7 Comparison of simulated altitude guidance solutions for several values of the bank angle limit, in a forward-look sensing scenario (R_{look} = 250 m). The target altitude h_c = 100 m.

In the early detection scenarios, the commanded altitude h_c is specified as 90 m; whereas for the reactive sensing cases, h_c is taken as 70 m. The specification of the previous command values has been based on a priori knowledge of the open-loop optimal solutions listed in Table 1.

Figure 5 shows guidance solutions for lateral escape in the absence of advance warning. Although the commanded altitude (70 m) is close to the open-loop optimal recovery altitude (80 m), the altitude guidance law does not have any problem tracking the commanded altitude throughout the high-shear region. Moreover, specific energy is well managed, as evidenced by the fact that the energy loss in the simulated altitude guidance solution is less than in the exact Chebyshev solution. Note that the Chebyshev solution features a somewhat undesirable behavior in the after-shear region. This is a consequence of the fact that no terminal boundary conditions have been specified, so that angle of attack remains on its limit until termination.[3]

Altitude guidance easily outperforms constant-pitch guidance in terms of both recovery altitude and energy management. A comparison with Fig. 3 reveals that the constant-pitch solution indeed closely agrees with a Bolza solution in terms of recovery altitude and overall trajectory behavior; albeit that minimum altitude is reached at a slightly later instance in the constant-pitch solution.

When the escape maneuver is confined to a vertical plane, the altitude guidance solution still manages to avoid running into the stick shaker limit within the high-shear region. In other words, a commanded altitude that is less than 5 m below the ideal recovery altitude can still be tracked. Results for these nonturning escape maneuvers can be found in Ref. 6.

Figure 6 shows results for simulated (lateral) guidance solutions for a scenario in which advance warning is considered. The reason for the superior performance of advance warning escape flights is demonstrated in Fig. 6c. Although only a few seconds of advance warning is considered in the present forward-look scenario, this is already sufficient to allow valuable energy to be gained before the microburst core is actually entered.

A few interesting observations can still be made. First of all, note that in contrast to the solution in the previously considered in situ detection scenario, the Chebyshev solution in the present scenario does not exhibit an immediate descent. In a Chebyshev solution, any energy gained prior to entry of the

microburst core is fully utilized to increase the recovery altitude. The actually achieved minimum airspeed in a Chebyshev solution is virtually the same for the in situ and forward-look sensing scenarios.

A close examination of the simulation results reveals that the constant-pitch technique does not fully exploit the potential to gain energy when the aircraft is still in the region of increasing headwind (i.e., $F < 0$). Early initiation of an escape executed with the constant-pitch technique enhances the initial tendency to climb, resulting in a penetration of the microburst core at a relatively high altitude. Consequently, the aircraft will actually be exposed to a higher downdraft than in the corresponding in situ detection scenario. In a manner different than the constant-pitch technique, no dramatic altitude excursions occur during an escape maneuver based on altitude guidance. Since large altitude excursions tend to raise the anxiety levels experienced by pilots,[6] the more docile escape maneuvers resulting from altitude guidance are probably more readily accepted by pilots. On the other hand, however, it needs to be noted that in comparison with altitude guidance, the constant-pitch technique does result in a (marginally) higher minimum airspeed during the recovery, at least, for the scenario's considered in this study.

The final guidance example involves altitude guidance only. The considered forward-look sensing scenario is exactly the same as in the previous example, except that the commanded altitude h_c has been increased from 90 to 100 m. Table 1 shows that a recovery altitude of that magnitude can be attained in a lateral escape, but not in a nonturning escape. The results for the nonturning and lateral escapes are shown in Fig. 7. For illustrative purposes, a lateral escape with a slightly larger bank angle limit has also been included ($\mu_{max} = 15$ deg). The effect of the increased commanded altitude is readily apparent. Without lateral maneuvering, the airspeed reserve is insufficient to withstand the energy drain caused by windshear and, as a result, angle of attack prematurely runs into its limit. Consequently, the commanded altitude cannot be followed throughout the recovery. The lateral escapes, on the other hand, succeed in limiting the energy loss, and recovery can take place at the desired altitude. Executing a lateral escape results in an improved management of specific energy, primarily because of the short-cut within the high-shear region (Fig. 7d).

VI. Implementation Aspects

As pointed out earlier in this paper, the major missing element that needs to be developed before a practical implementation of altitude guidance can take place, is the logic for determining the attainable recovery altitude. Although the objective is to select this altitude as high as possible, based on in situ wind information only, it is simply not possible to a priori predict up to which altitude a safe recovery can be made. Indeed, the successful development of such logic for application in a closed-loop guidance scheme hinges upon the ability to produce a realistic estimate of the total windshear-induced energy loss. When a long-range forward-look sensor is used (capable of probing the spatial extent of the microburst), such an estimation is probably possible, albeit that the prediction of the evolution of the aircraft state (speed/altitude) during the windshear exposure remains an inherent source of uncertainty. For short-range forward-look sensing, the prediction of energy reduction resulting from windshear exposure is even more challenging. Perhaps an attempt can be made to relate the commanded recovery altitude to the energy gain prior to core penetration, and then to adapt the commanded altitude as the recovery unfolds. In any case, it is clear that much further research is needed to develop this type of intelligent controller.

Because of the recent advances made in the area of forward-looking windshear detection and warning systems, alert times of up to 90 s can be obtained in an impending microburst encounter.[6] Clearly, alert times of this magnitude allow a pilot on final approach to totally avoid the microburst, simply by executing a go-around in a timely fashion. In view of the fairly large warning times offered by advanced detection and warning systems, one may wonder whether there is a real need for escape guidance strategies. However, as evidenced by some recent windshear accidents,[11] a microburst may form and dissipate within a relatively short time span. Consequently, the need for guidance strategies is likely to remain, even if long-range forward-looking systems are employed.

A very important aspect is the availability and quality of the wind information used in the proposed feedback guidance scheme. The sensors to measure the required information may include the usual air data instruments and inertial sensors (IRS), as well as advanced systems for predictive detection and warning (like lidar or radar). Two important wind-related quantities must be estimated on-line, viz., the F-factor and the relative wind direction. Fairly accurate and reliable F-factor algorithms/systems have been available for several years.[6] However, the use of the relative wind direction for feedback purposes has not been widely examined. Reference 6 presents a preliminary investigation on the real-time estimation of the relative wind direction, for both reactive and predictive systems.

At first glance, it may appear that the estimation of the relative wind direction is not very critical. In the initial headwind phase, prior to entry of the core, the relative wind angle will usually be so large that the guidance law [Eq. (18)] will call for a maximum bank angle. Moreover, simulation experiments have shown that the performance solution is not very sensitive with respect to debanking behavior. What is important is that the aircraft does not make a turn in the wrong direction; i.e., a turn toward the microburst center. As already shown in Ref. 2, turning in the wrong direction may have dramatic consequences with regard to recovery altitude. The scenarios considered in this report all assume a symmetric encounter and, therefore, it makes no difference whether a left or a right turn is executed. When the center of the microburst is laterally offset from the runway centerline extension, the choice of turn direction becomes important. The turn should always be executed in the same direction as the crosswind. The stronger the experienced crosswind component, the more critical it is that the choice of turn direction is correct. It can thus be concluded that the relative wind direction must be estimated with some degree of accuracy. The question is whether in a real-world situation, the estimated wind direction (or wind vector components) is not corrupted too much by high-frequency turbulence signals. Indeed, we have to remain aware of the fact that in the simulations, highly idealized (axisymmetric) windshear models are used. In reality, spatial wind variations will generally exhibit a far more erratic behavior than the simple models suggest. Several techniques have been proposed that promise accurate estimates of wind components, as well as their time derivatives, from the output of in situ sensors.[12,13] Currently, it is under investigation whether these techniques are suitable for lateral guidance purposes.

Another real concern that has not yet been addressed relates to the occurrence of multiple simultaneous microbursts, possibly in different stages of their development (temporal wind variations). Indeed, the in situ detection of a microburst may trigger a lateral escape, only to find out that the aircraft is turning toward the center of a second, perhaps even stronger, microburst located slightly further down the approach route. Of course, a more optimistic scenario, for example, escaping from one microburst while avoiding another in the process, is just as probable. Evidently, this does not take away the fact that we do not wish the outcome of an encounter to be determined by chance. An investigation of detection and guidance in a complex wind flowfield is clearly warranted, obviously with due consideration to the probability of occurrence of such events.

VII. Conclusions

In this paper, a preliminary study on the development of a new microburst escape guidance strategy has been presented

that includes lateral maneuvering. Both in situ (reactive) and short-range forward-look (predictive) sensing of windshear was simulated. Based on a comparison with exact Chebyshev solutions, it can be concluded that the simulated guidance solutions demonstrated a very satisfactory performance in terms of recovery altitude and energy management. The simulation results confirmed the earlier observations that a lateral escape is particularly effective in improving the recovery performance if advance warning is provided. It can thus be concluded that by permitting lateral escape strategies, forward-look sensor requirements can be reduced, which evidently translates into improved economic viability of forward-look systems.

The employed altitude guidance technique was shown to be fairly robust with respect to uncertainty in the microburst strength, without any real sacrifices in terms of recovery altitude. However, a predictive logic for determining the best recovery altitude is an important element that is still missing. The development of appropriate logic for determining the recovery altitude is the first step to be taken, before the practicality of the altitude guidance technique can be further assessed.

References

[1]Miele, A., Wang, T., Melvin, W. W., and Bowles, R. L., "Acceleration, Gamma and Theta Guidance for Abort Landing in a Windshear," *Journal of Guidance, Control, and Dynamics*, Vol. 12, No. 6, 1989, pp. 815–821.

[2]Visser, H. G., "Optimal Lateral-Escape Maneuvers for Microburst Encounters During Final Approach," *Journal of Guidance, Control, and Dynamics*, Vol. 17, No. 6, 1994, pp. 1234–1240.

[3]Visser, H. G., "A Minimax Optimal Control Analysis of Lateral Escape Maneuvers for Microburst Encounters," *Journal of Guidance, Control, and Dynamics*, Vol. 20, No. 2, 1997, pp. 370–376.

[4]Visser, H. G., "Optimal Lateral Maneuvering for Microburst Encounters During Final Approach," *Proceedings of the 18th ICAS Congress* (Bejing), AIAA, Washington, DC, 1992, pp. 1587–1597.

[5]Zhao, Y., and Bryson, A. E., "Optimal Paths Through Downbursts," *Journal of Guidance, Control, and Dynamics*, Vol. 13, No. 5, 1990, pp. 813–818.

[6]Visser, H. G., "Lateral Escape Guidance Strategies for Microburst Windshear Encounters," Delft Univ. of Technology, M-723, Delft, The Netherlands, 1996.

[7]Mulgund, S. S., and Stengel, R. F., "Aircraft Flight Control in Wind Shear Using Sequential Dynamic Inversion," *Journal of Guidance, Control, and Dynamics*, Vol. 18, No. 5, 1995, pp. 1084–1091.

[8]Isodori, A., "Nonlinear Control Systems: An Introduction," *Lecture Notes in Control and Information Sciences*, Springer–Verlag, Berlin, 1985.

[9]*Windshear Training Aid*, U.S. Dept. of Transportation, Federal Aviation Administration, Washington, DC, 1987.

[10]Mulgund, S. S., and Stengel, R. F., "Target Pitch Angle for the Microburst Escape Maneuver," *Journal of Aircraft*, Vol. 30, No. 6, 1993, pp. 826–832.

[11]Phillips, E. H., "Crash Probe Focuses on Severe Microburst," *Aviation Week & Space Technology*, Sept. 26, 1994.

[12]Mulgund, S. S., and Stengel, R. F., "Optimal Nonlinear Estimation for Aircraft Flight Control in Wind Shear," *Automatica*, Vol. 32, No. 1, 1996, pp. 3–13.

[13]Miele, A., Wang, T., and Melvin, W. W., "Real-Time Wind Identification Technique," William Marsh Rice Univ., Aero-Astronautics Rept. 256, Houston, TX, 1991.